

A study of Kepler supernova remnant: angular power spectrum estimation from radio frequency data

Preetha Saha,¹ Somnath Bharadwaj,¹ Nirupam Roy,² Samir Choudhuri,³ Debatri Chattopadhyay⁴

¹ Department of Physics and Centre for Theoretical Studies, Indian Institute of Technology, Kharagpur 721302, India

² Department of Physics, Indian Institute of Science, Bangalore 560012, India

³ National Centre for Radio Astrophysics, Tata Institute of Fundamental Research, Pune University campus, Pune 411 007, India

⁴ Centre for Astrophysics and Supercomputing, Swinburne Institute of Technology, John St, Hawthorn, Victoria 3122, Australia

preetha@phy.iitkgp.ernet.in



Abstract

Supernova remnants (SNRs) have a variety of overall morphology as well as rich structures over a wide range of scales. Quantitative study of these structures can potentially reveal fluctuations of density and magnetic field originating from the interaction with ambient medium and turbulence in the expanding ejecta. We have used 1.5GHz (L band) and 5GHz (C band) VLA data to estimate the angular power spectrum C_ℓ of the synchrotron emission fluctuations of the Kepler SNR. This is done using the novel, visibility based, Tapered Gridded Estimator of C_ℓ .

Introduction

At radio wavelengths, the dominant contribution to the SNR emission comes from the non-thermal synchrotron radiation. The interaction between the ISM and the ejecta amounts to a convective instability, which accounts for the observed synchrotron radio emission.

- We want to estimate the angular power spectrum C_ℓ of observed intensity fluctuations of Kepler SNR using VLA archival visibility data (AD498) observed in 1.5GHz (L band) and 5GHz (C band).
- Tapered Gridded Estimator (TGE) [1] helps in computing the angular power spectrum directly from the visibilities by efficiently gridding the data, thereby reducing the computational time.
- We also present C_ℓ estimates of Cas A and Crab as consistency checks for the estimator and to verify the results reported in [2].

Methodology

Power spectrum estimation using TGE

- The visibility based TGE (details in [3, 1]) applied to the calibrated visibility data of the SNR to estimate C_ℓ .
- The sky is tapered by multiplying with a frequency independent window function $W(\theta) = e^{-\theta^2/\theta_w^2}$.
- Tapering suppresses the contribution from the outer region of the telescope's field of view (FoV).

$$\mathcal{V}_{cg} = \sum_i \tilde{w}(U_g - U_i) \mathcal{V}_i \quad (1)$$

where $\tilde{w}(U)$ is the Fourier transform of the taper window function $W(\theta)$ and U_g refers to the corresponding baseline of the grid point.

- The estimator is defined as

$$\hat{E}_g = (M_g)^{-1} \times \left(|\mathcal{V}_{cg}|^2 - \sum_i |\tilde{w}(U_g - U_i)|^2 |\mathcal{V}_i|^2 \right) \quad (2)$$

where M_g is the normalization constant and $\langle \hat{E}_g \rangle$ gives an unbiased estimate of C_ℓ at the angular multipole $\ell_g = 2\pi U_g$.

- The circular bin averaged values of C_ℓ referred as C_ℓ^E .

Interpreting C_ℓ^E

- The specific intensity fluctuation $\delta I(\theta)$ of the radiation received from the SNR modelled through

$$\delta I(\theta) = R(\theta) [\bar{I}_s + \delta I_s(\theta)] \quad (3)$$

where \bar{I}_s is a mean uniform intensity and $\delta I_s(\theta)$ is a fluctuating component.

- $\delta I_s(\theta)$ assumed to be the outcome of a statistically homogeneous and isotropic Gaussian random process (presumably turbulence) whose statistical properties are completely specified by C_ℓ .
- The C_ℓ^E estimated from $\delta I(\theta)$ is related to C_ℓ (which corresponds to $\delta I_s(\theta)$) through a convolution

$$C_{2\pi|U|}^E = \int d^2U' |\tilde{r}(U - U')|^2 C_{2\pi|U'|} \quad (4)$$

where $\tilde{r}(U)$ is the Fourier transform of profile function $R(\theta)$.

- The angular profile of the SNR modelled as a Gaussian of the form $R(\theta) = e^{-\theta^2/\theta_r^2}$.
- The value of θ_r chosen so as to correctly reproduce the break ℓ_m in C_ℓ^E .

Error estimation

- The statistical fluctuations inherent to the sky signal $\mathcal{S}(U_i)$ as well as the system noise contribution \mathcal{N}_i both contribute to statistical errors δC_ℓ in C_ℓ^E .
- Several statistically independent realizations of the visibilities \mathcal{V}_i simulated for which the average C_ℓ matches C_ℓ^E .
- The variance determined from the multiple realizations of the simulation used to estimate the statistical errors δC_ℓ in the estimated C_ℓ^E .

Cas A and Crab revisited

The angular power spectrum C_ℓ^E of Cas A and Crab SNR obtained using TGE are broadly consistent with the earlier results of [2].

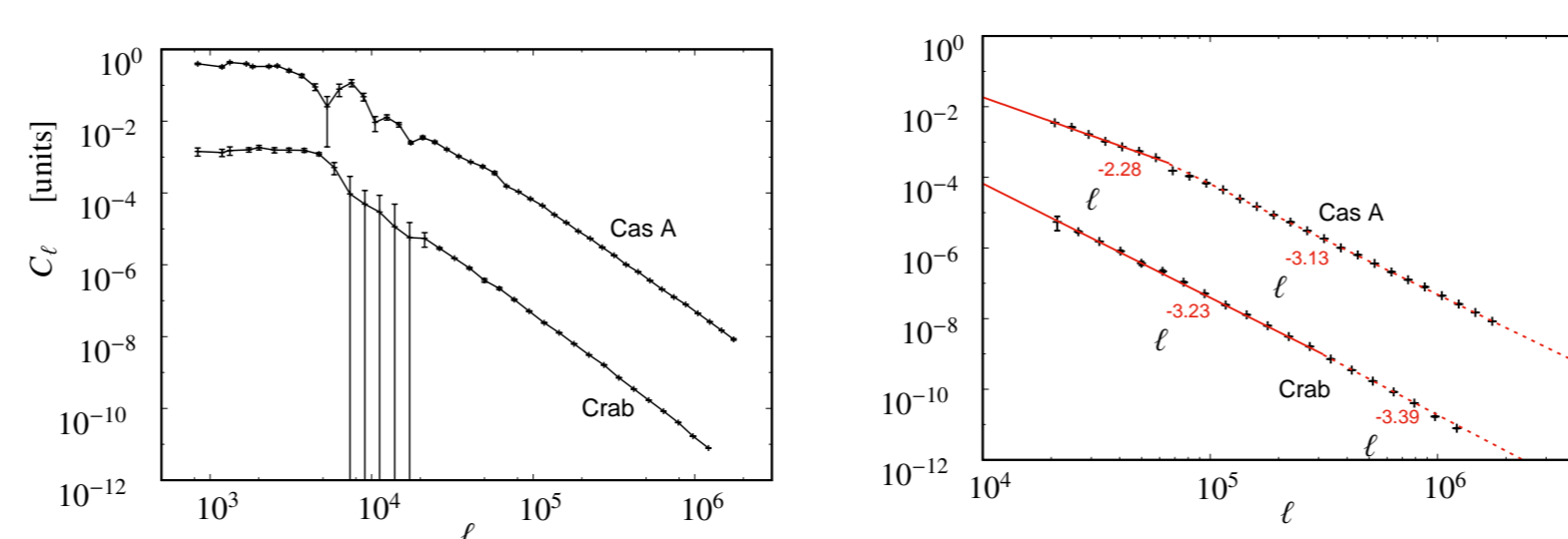


Figure 1: C_ℓ^E of Cas A and Crab SNRs as a function of angular multipole ℓ with $\pm 1\sigma$ error bars. The amplitude of C_ℓ^E of Cas A and Crab SNRs is arbitrarily set for clarity. The convolution dominated region for $\ell < 10^4$ has not been shown in the right panel. The best fit lines are plotted with red solid and dot lines in the right panel.

Results

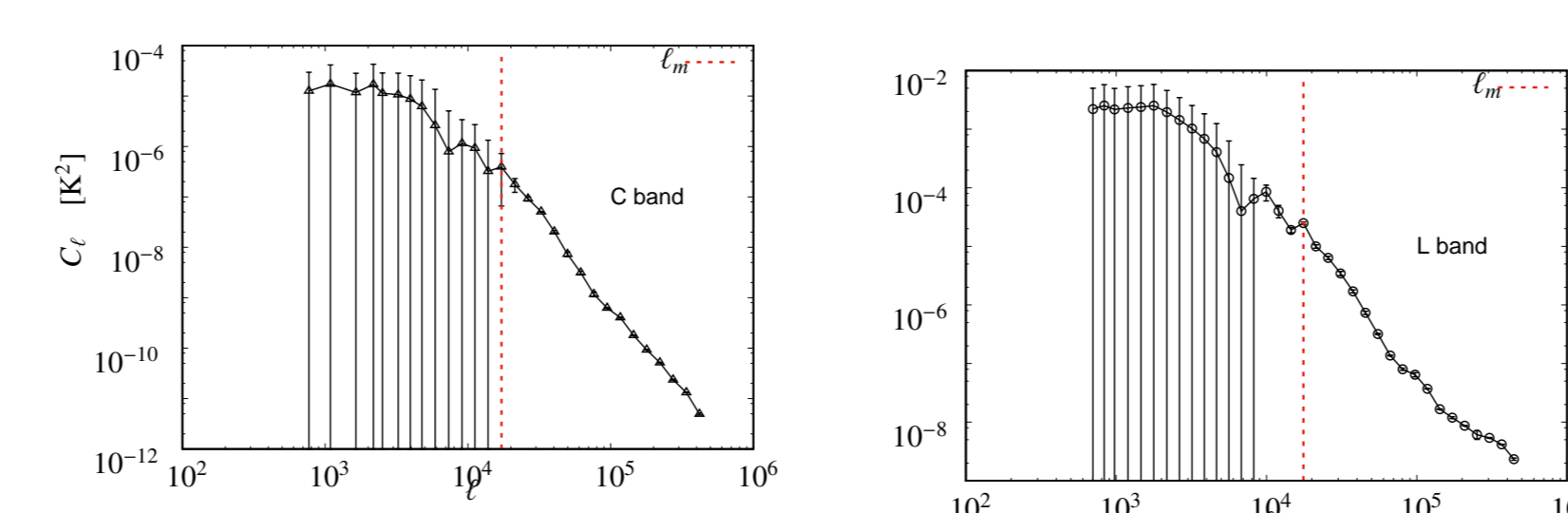


Figure 2: C_ℓ^E of Kepler SNR as a function of angular multipole ℓ with $\pm 1\sigma$ error bars.

- The value of ℓ_m is inversely proportional to the angular extent of the SNR, the exact value of ℓ_m however depends on the slope β and the shape of the profile function $R(\theta)$.

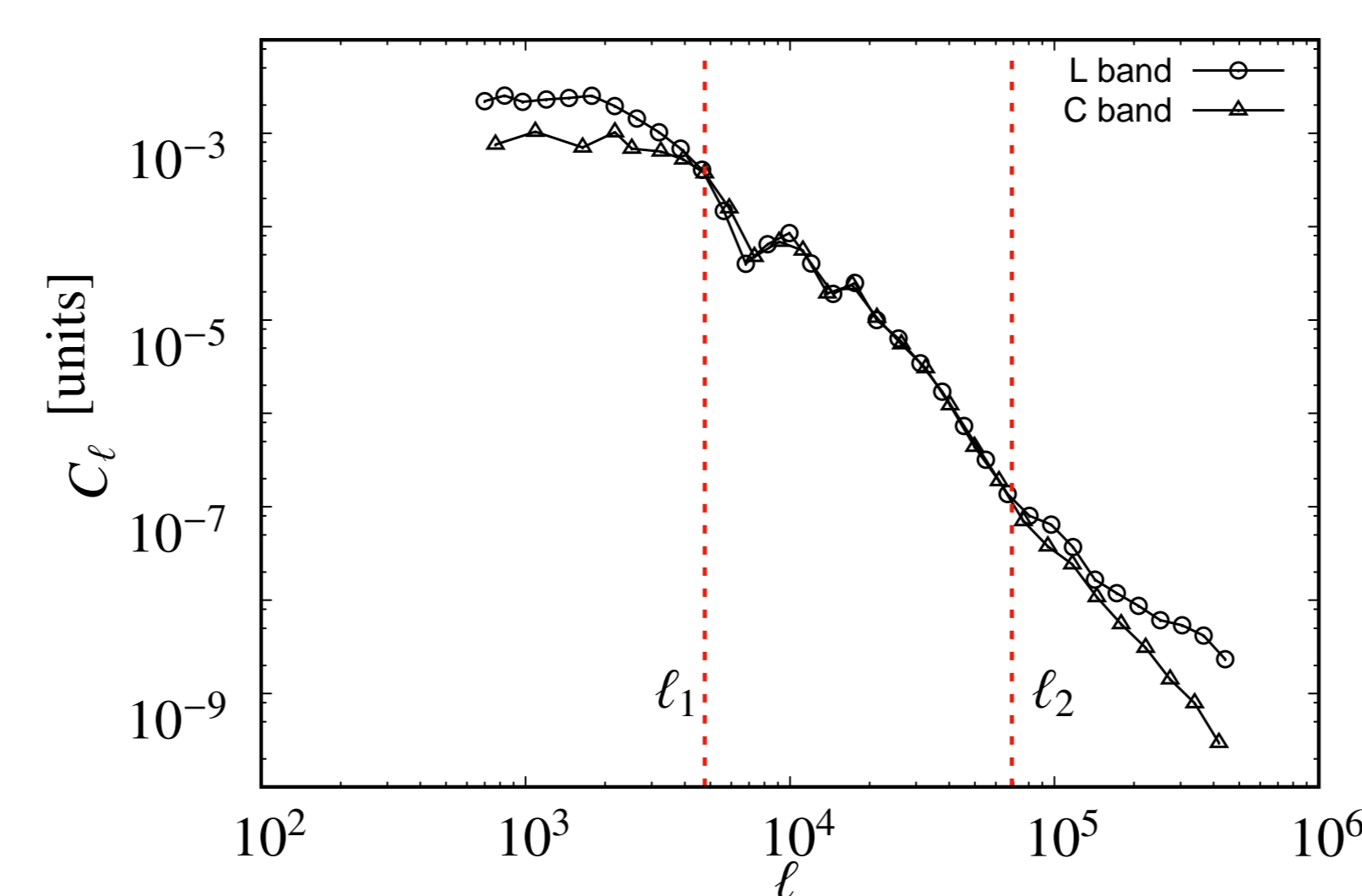


Figure 3: C_ℓ^E of Kepler SNR for C and L bands in arbitrary units, without the 1σ error bars.

- The kink like features seen in the C and L bands match with respect to both the ℓ position as well as the relative amplitude.
- The C and L band results are in close agreement over a broad ℓ range $\ell_1 = 4.76 \times 10^3$ to $\ell_2 = 6.91 \times 10^4$.
- The close match between C and L band results reinforces that C_ℓ^E reflects genuine astrophysical features pertaining to Kepler SNR.

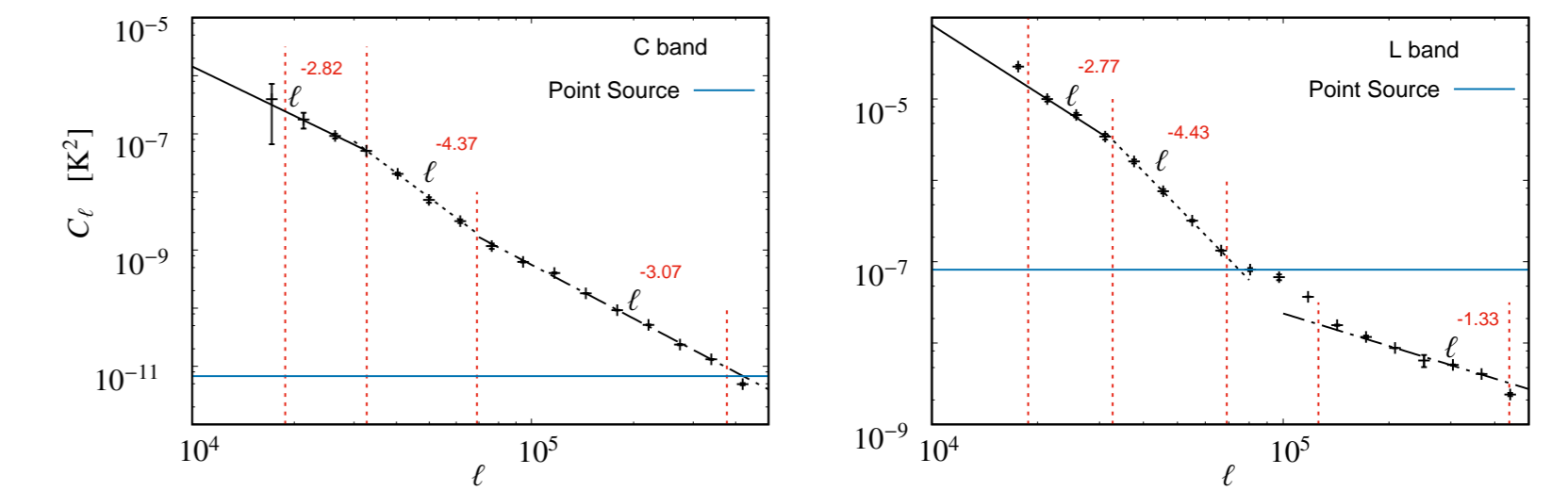


Figure 4: C_ℓ^E of Kepler SNR as a function of angular multipole ℓ , for $\ell > 10^4$. The best fit lines are plotted in black solid line, dot line and dot-dash line for the three ℓ ranges (demarcated by vertical red dot lines) respectively.

- Used χ^2 minimization to fit power-law of the form $C_\ell = A\ell^\beta$ for $\ell > \ell_m$
- For $\ell = (1.9 - 6.9) \times 10^4$, the power spectrum is a broken power law with a break at $\ell = 3.3 \times 10^4$
- Power law index of -2.84 ± 0.07 and -4.39 ± 0.04 before and after the break respectively
- The break interpreted to be the shell thickness of the SNR (0.35 pc) which approximately matches $\ell = 3.3 \times 10^4$ (i.e., 0.48 pc or $0.33'$).
- For $\ell > 6.9 \times 10^4$, C_ℓ^E of L band likely to have dominant contribution from the foregrounds like extragalactic point sources or diffuse Galactic synchrotron emission or both and excluded from further discussion.

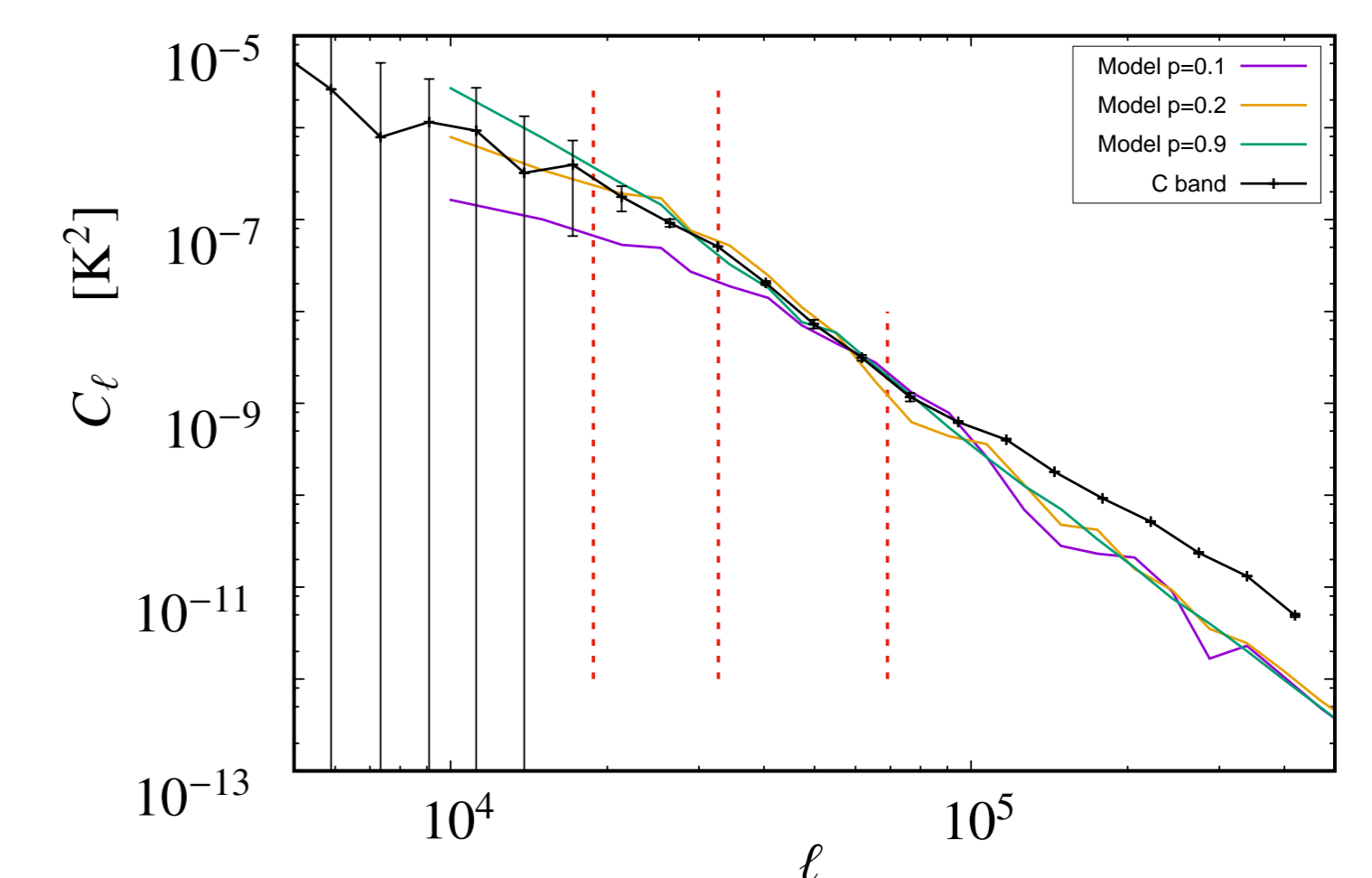


Figure 5: Comparison of C band C_ℓ^E (for $\ell > \ell_m$) of Kepler SNR with the simulated models of varying shell thickness t of the remnant. Here, $p = \frac{t}{r_{out}}$ where $r_{out} = 1.5'$, the angular radius of the remnant.

- For L band also, the transition angular scale from $\beta = -2.8$ to -4.4 of Kepler SNR agrees with the model $p = 0.2$.
- This supports the interpretation of the shell thickness derived from the results.

Conclusions

- We have interpreted the intensity fluctuations of the Kepler SNR as arising from MHD turbulence.
- At large angular scales the slope ($\beta = -2.8$) is consistent with 2D Kolmogorov turbulence and also the angular two-point correlation of the Tycho SNR [4].
- At small angular scales the slope ($\beta = -3.1$) is consistent with earlier measurements for Cas A and Crab SNRs [2].
- The third intermediate ℓ range where the power spectrum falls steeply with $\beta = -4.4$ has not been observed in any of the three SNRs analyzed earlier and this is possibly an outcome of the complex morphology of Kepler SNR.

References

- [1] S. Choudhuri, S. Bharadwaj, S. Chatterjee, S. S. Ali, N. Roy, and A. Ghosh. The visibility-based tapered gridded estimator (TGE) for the redshifted 21-cm power spectrum. *MNRAS*, 463:4093–4107, December 2016.
- [2] N. Roy, S. Bharadwaj, P. Dutta, and J. N. Chengalur. Magnetohydrodynamic turbulence in supernova remnants. *MNRAS*, 393:L26–L30, February 2009.
- [3] S. Choudhuri, S. Bharadwaj, A. Ghosh, and S. S. Ali. Visibility-based angular power spectrum estimation in low-frequency radio interferometric observations. *MNRAS*, 445:4351–4365, December 2014.
- [4] Jiro Shimoda, Takuya Akahori, A. Lazarian, Tsuyoshi Inoue, and Yutaka Fujita. Discovery of Kolmogorov-like magnetic energy spectrum in Tycho's supernova remnant by two-point correlations of synchrotron intensity. *MNRAS*, 480:2200–2205, October 2018.